Fabrication of silicon heterojunction solar cells with a boron-doped a-Si:H layer formed by catalytic impurity doping

Cite as: AIP Advances 9, 115013 (2019); doi: 10.1063/1.5123769
Submitted: 9 August 2019 • Accepted: 2 November 2019 •
Published Online: 15 November 2019

Katsuya Akiyama and Keisuke Ohdaira[a)]

AFFILIATIONS

Japan Advanced Institute of Science and Technology (JAIST), 1-1 Asahidai, Nomi, Ishikawa 923-1292, Japan

[a)]**Author to whom correspondence should be addressed:** ohdaira@jaist.ac.jp. **Tel.:** +81-761-51-1563.

ABSTRACT

We investigate the effect of boron (B) catalytic impurity doping (Cat-doping), a low-temperature doping method by exposing to catalytically generated dopant radicals, on hydrogenated amorphous silicon (a-Si:H) films and the influence of the electrical properties of indium tin oxide (ITO) films on the tunneling conduction of carriers through the ITO/a-Si:H interfaces. The usage of ITO films with higher carrier density and B Cat-doped a-Si:H films formed with the addition of H_2 enhances carrier tunneling through the a-Si:H/ITO interfaces. We also evaluate the current density–voltage (J–V) characteristics of Si heterojunction (SHJ) solar cells with a B Cat-doped a-Si:H layer as an emitter layer. In the case of B Cat-doping with the addition of H_2, we obtain a SHJ solar cell which shows a conversion efficiency (η) of 12.6% and an open-circuit voltage (V_{oc}) of 617 mV. The postannealing of the SHJ cells is effective to improve their V_{oc} and η. These results will lead to the application of B Cat-doping on heterojunction back-contact solar cells in the future.

I. INTRODUCTION

Photovoltaic (PV) technology has been developed as alternative energy to fossil fuel, and solar cells based on crystalline silicon (c-Si) wafers are being the most commercialized ones in the PV market. In recent years, Si heterojunction (SHJ) solar cells, consisting of hydrogenated amorphous Si (a-Si:H)/c-Si heterojunctions, have attracted attention, owing to their high conversion efficiency originating from the high-quality passivation of c-Si surfaces by a-Si:H films.[1–7] In particular, heterojunction back-contact (HBC) solar cells, in which all the electrodes and p–n junctions are formed on the rear side, exhibit extremely high conversion efficiencies due to the reduction of optical loss as well as the good surface passivation, and a HBC solar cell with a conversion efficiency of 26.7% has been demonstrated very recently.[8] However, the fabrication of HBC solar cells, in general, requires more process steps than conventional SHJ cells, particularly for the patterning of doped a-Si:H films and metal electrodes. This increases their process cost and is thus a critical issue for the industrialization of the HBC cells. Simple patterning methods for the fabrication of HBC cells will therefore be needed.

Catalytic impurity doping (Cat-doping)[9–17] is a doping method of exposing Si samples to boron (B) or phosphorus (P)-related radicals generated through catalytic reaction on a heated catalyzing wire in a catalytic chemical vapor deposition (Cat-CVD)[18–24] apparatus. B or P Cat-doping can form an ultrathin (~10 nm) doping layer on a c-Si surface, which can provide field-effect passivation and effectively suppress the surface recombination of minority carriers on the Si surface.[9,10,12–14] It should be emphasized that Cat-doped layers can be formed at temperatures below 200 °C and do not require any additional postannealing for the activation of the introduced dopants. Cat-doping can thus be utilized for the fabrication process of SHJ solar cells.[13] Cat-doping is applicable not only to c-Si wafers but also to a-Si:H films: intrinsic a-Si:H (i-a-Si:H) films can be converted to *p*-type a-Si:H (p-a-Si:H) or *n*-type a-Si:H (n-a-Si:H) films.[16,17] B and P atoms in a Cat-doped a-Si:H layer exist in the vicinity of the surface (~10 nm), and p/i or n/i a-Si:H stacks can be easily formed by exposing ~20 nm-thick i-a-Si:H to catalytically generated B- or P-related radicals.[16] If the partial formation of doped a-Si:H films is realized by Cat-doping, e.g., through a hard mask, it can be a simple patterning method for the fabrication of HBC

TABLE I. Conditions for B Cat-doping and the formation of a-Si:H and ITO films for the evaluation of the electrical properties of ITO/a-Si:H stacks.

						Gas flow rate (SCCM)			
	T_{holder} (°C)	T_{cat} (°C)	RF power (W)	Duration	Pressure (Pa)	SiH_4	He:B_2H_6 (2.25%)	H_2	Ar
i-a-Si:H	125	1800	...	90 s	1	10	...	...	...
B Cat-doping	350	1800	...	600 s	3.9	...	20	0, 20	...
ITO	100, 200	...	50	27 min	0.5	...	...	...	13.7

cells.[25] We have thus far demonstrated the operation of a SHJ solar cell containing a B Cat-doped a-Si:H layer with a conversion efficiency of 6.28% [a short-circuit current density (J_{sc}) of 27.5 mA/cm^2, an open-circuit voltage (V_{oc}) of 402 mV, and a fill factor (FF) of 0.568].[17] The performance of the SHJ cell with a B Cat-doped a-Si:H emitter is much worse than conventional ones with a deposited p-a-Si:H film. This may be due to the imperfect electrical characteristics of a-Si:H/ITO interfaces and insufficient B concentration in the B Cat-doped a-Si:H, particularly for such low values of V_{oc} and FF. More built-in potential may be needed for an increase in V_{oc}, and more effective tunneling conduction of carriers through the ITO/B Cat-doped a-Si:H is necessary for higher FF.

In this work, we investigate the effect of B Cat-doping on the tunneling conduction of carriers through ITO/a-Si:H interfaces for application to SHJ solar cells. The conditions of ITO deposition and B Cat-doping are systematically changed. We also fabricate and characterize SHJ solar cells with a B Cat-doped a-Si:H layer and demonstrate a SHJ cell with V_{oc} > 600 mV.

II. EXPERIMENTAL METHODS

A. Electrical properties of ITO/a-Si:H stacks

a-Si:H films with a thickness of ~16 nm were deposited on 20 × 20 × 0.3 mm^3-sized *p*-type c-Si substrates with a resistivity of 0.01–0.1 Ω cm by Cat-CVD under the conditions summarized in Table I. c-Si substrates were immersed in 5 wt. % HF for 30 s and then in 4 wt. % H_2O_2 for 30 s to prevent epitaxial growth during the a-Si:H deposition.[26] The a-Si:H samples were put in 30 wt. % H_2O_2 for 10 min immediately after the a-Si:H deposition to prevent the etching of a-Si:H films during Cat-doping, in which a large number of H radicals exist in vapor phase. B Cat-doping was conducted on the a-Si:H films under the conditions summarized in Table I, in which the H_2 flow rate was systematically changed. Note that an actual substrate temperature is ~200 °C in the case of a holder temperature (T_{holder}) of 350 °C. The a-Si:H samples after B Cat-doping were then immersed in 5 wt. % HF for 30 s to remove oxide layers on the surface. Indium tin oxide (ITO) films were deposited at 100 or 200 °C by sputtering on the a-Si:H films, and Al electrodes were formed by thermal evaporation on both sides of the samples. Finally, the samples were annealed in a furnace for 7 h under N_2 atmosphere to form an ohmic contact between c-Si and Al. The current density–voltage (*J*–*V*) characteristics of the samples were measured using a semiconductor parameter analyzer. The schematic of the completed samples is shown in Fig. 1. In this structure, a tunneling current flows through the ITO/B Cat-doped a-Si:H interface particularly under the negative bias application. We also fabricated and characterized the samples without ITO films for comparison to confirm that the a-Si:H/ITO interfaces limit the *J*–*V* characteristics of the samples. The electrical properties of ITO films were separately characterized by the Hall effect measurement using ITO films directly formed on glass substrates.

B. SHJ solar cells with a B Cat-doped a-Si:H layer

c-Si substrates were immersed in 5 wt. % HF for 30 s and in 4 wt. % H_2O_2 for 30 s, as mentioned in Sec. II A. i-a-Si:H films with a thickness of ~10 and ~16 nm were then deposited on the rear and the front sides, respectively, of 20 × 20 × 0.26–0.3 mm^3-sized *n*-type c-Si substrates with a resistivity of 1–5 Ω cm by Cat-CVD under the conditions summarized in Table II. The a-Si:H samples were immersed in 30 wt. % H_2O_2 for 10 min immediately after the a-Si:H deposition, as also mentioned in Sec. II A.[26] B Cat-doping was conducted on the 16 nm-thick a-Si:H films under the conditions summarized in Table II, in which the H_2 flow rate was changed. To confirm the presence or absence of the deposition of a-Si:H, e.g., from the chamber wall, during B Cat-doping, bare quartz glass substrates were exposed to B Cat-doping and their optical transmittance spectra were measured. After the samples receiving B Cat-doping were immersed in 5 wt. % HF for 30 s, 7 nm-thick n-a-Si:H films were deposited on 10 nm-thick i-a-Si:H films by Cat-CVD. Because a few hours have passed since the deposition of n-a-Si:H films, the samples were again immersed in 5 wt. % HF for 30 s, and 77 nm-thick ITO films were then deposited on both sides of the samples by sputtering under the conditions summarized in Table II. Comb-shaped Ag electrodes were printed on both sides of the samples by

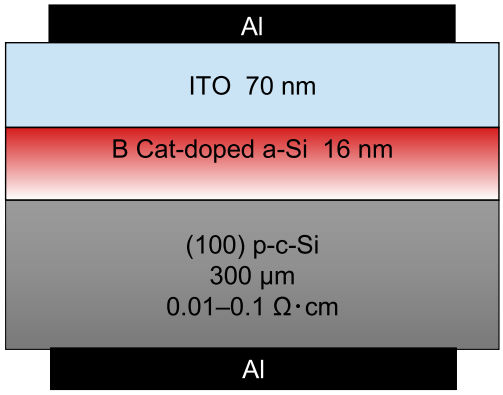

FIG. 1. Schematic of an ITO/B Cat-doped a-Si:H/c-Si structure.

TABLE II. Conditions for B Cat-doping and the formation of a-Si:H and ITO films for the fabrication of SHJ cells.

						Gas flow rate (SCCM)				
	T_{holder} (°C)	T_{cat} (°C)	RF power (W)	Duration	Pressure (Pa)	SiH_4	He:B_2H_6 (2.25%)	He:PH_3 (2.25%)	H_2	Ar
i-a-Si:H	125	1800	...	45, 90 s	1	10	...	...	...	...
B Cat-doping	350	1800	...	600 s	3.9	...	20	...	0, 20	...
n-a-Si:H	250	1800	...	35 s	2	10	...	4.4	...	...
ITO	200	...	50	27 min	0.5	...	...	...	...	13.7

screen printing and then the samples were annealed at 200 °C for 1 h in air. The schematic of the SHJ cells is shown in Fig. 2. We also fabricated a SHJ solar cell without a *p*-type emitter layer as a reference sample to clearly observe the effect of B Cat-doping on i-a-Si:H on the device performance. The *J*–*V* characteristics of the SHJ cells were measured under air mass 1.5 light illumination with an irradiance of 100 mW/cm^2 from the p-a-Si:H side. In addition, the completed SHJ solar cells with a B Cat-doped a-Si:H layer were annealed at 200 °C for 5–20 h in air, and the *J*–*V* characteristics were measured after the postannealing.

III. RESULTS AND DISCUSSION

A. Tunneling conduction through a-Si:H/ITO interfaces

Figure 3 shows the *J*–*V* characteristics of the Al/B Cat-doped a-Si:H/p-c-Si/Al structure fabricated as a reference sample. These samples show linear *J*–*V* characteristics. The conductivity of B Cat-doped a-Si:H films was 5.3 × 10^{-10} S/cm^2. Hence, in this sample structure, linear *J*–*V* characteristics are obtained even for B Cat-doped a-Si:H with such a low conductivity. We have also separately confirmed that Al/ITO contacts are ohmic. The electrical properties of the ITO films deposited at 100 and 200 °C, evaluated by the Hall effect measurement, are summarized in Table III. The resistivities of ITO films are sufficiently low (~10^{-4} Ω cm), which do not limit the overall resistivity of the samples. Therefore, the *J*–*V* characteristics of the samples, whose structure is described in Fig. 1, are limited solely by the tunneling conduction through the a-Si:H/ITO interface.

Figure 4 shows the *J*–*V* characteristics of ITO/B Cat-doped a-Si:H/p-c-Si/Al structures, together with those of the samples receiving no B Cat-doping for comparison. The structures with B Cat-doping show larger conductivity than those without B Cat-doping. Furthermore, it is suggested that the usage of ITO films deposited at 200 °C leads to a larger tunneling current. The carrier concentration in ITO films is increased by preparing the films at a higher temperature, as summarized in Table III. Similar tendency has also been reported by Kim *et al.*[27] This may explain the improvement in the tunneling conduction by using ITO films prepared at a higher temperature. More carrier density in the ITO films, in other words, a higher Fermi level position with respect to the conduction band edge

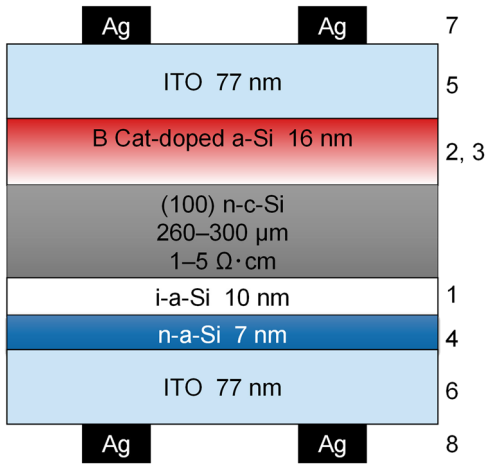

FIG. 2. Schematic of a SHJ solar cell with a B Cat-doped a-Si:H layer. The numbers on the right hand side of the figure indicate the order of the fabrication process.

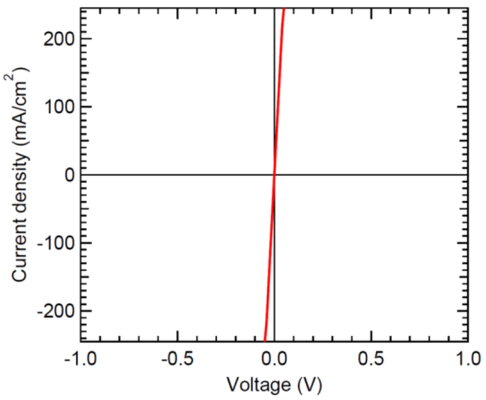

FIG. 3. *J*–*V* characteristics of Al/B Cat-doped a-Si:H/p-c-Si/Al structures.

TABLE III. Electrical properties of ITO films.

T_{holder} (°C)	Resistivity (Ω cm)	Mobility (cm^2/Vs)	Carrier density (cm^{-3})
100	1.9 × 10^{-4}	10.9	3.0 × 10^{21}
200	1.0 × 10^{-4}	11.5	5.5 × 10^{21}

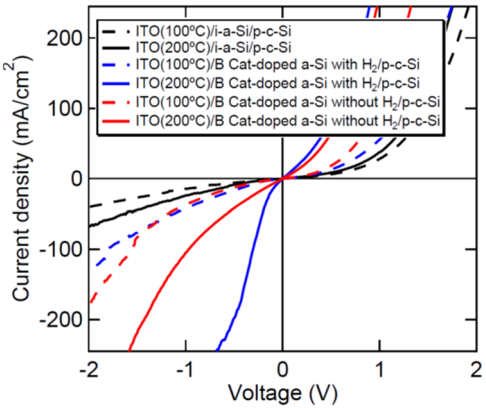

FIG. 4. *J–V* characteristics of ITO/B Cat-doped a-Si:H/p-c-Si structures. *J–V* characteristics of the samples without B Cat-doping are also shown for comparison.

of ITO, improves the tunneling of carriers through the interface. The addition of H_2 during B Cat-doping on a-Si:H films also enhances the tunneling conduction. This is reasonable since the conductivity of an a-Si:H film B Cat-doped with H_2 addition is 1.3×10^{-7} S/cm, which is much larger than that of an a-Si:H film B Cat-doped without H_2 addition of 1.0×10^{-8} S/cm.[16]

B. SHJ solar cells with a B Cat-doped a-Si:H layer

Figure 5 shows the *J–V* characteristics of SHJ solar cells without and with a B Cat-doped a-Si:H layer with and without the addition of H_2 during B Cat-doping. We fabricated a SHJ solar cell without a *p*-type emitter layer as well, the *J–V* characteristics of which are also shown in Fig. 5. The areas for the SHJ solar cells of the blue, red, and black lines in Fig. 5 are 0.89, 1.73, and 1.83 cm^2, respectively, in which the area of Ag electrodes is not included. A SHJ solar cell without a *p*-type emitter layer shows the photovoltaic effect, as also reported by Fujiwara *et al.*[28] The junction between *n*-type c-Si and intrinsic a-Si:H may work like a p–n junction. B Cat-doping forms a *p*-type emitter layer on the a-Si:H surface, and the B Cat-doped layer highly improves V_{oc} and FF. V_{oc} and FF are increased more effectively by B Cat-doping in the case of adding H_2 during B Cat-doping. This is probably because of improved doping efficiency[16] resulting from more effective decomposition of B_2H_6 molecules through vapor phase reaction with H radicals.[29] The improvement in V_{oc} may indicate the enlargement of built-in potential in the p–n junction, and the improvement in FF is probably due to more efficient carrier tunneling through the a-Si:H/ITO interfaces.

Figure 6 shows the optical transmittance spectra of quartz glass substrates before and after exposure to B Cat-doping. One can see no significant change in the transmittance spectra by B Cat-doping. This clearly indicates that the deposition of p-a-Si:H from a chamber wall did not occur during B Cat-doping, and the improvement in the performance of SHJ solar cells is owing to the doping of B atoms on i-a-Si:H films.

Figures 7(a)–7(d) show η, J_{sc}, V_{oc}, and FF of SHJ solar cells with a B Cat-doped a-Si:H layer as a function of postannealing duration. η increased by postannealing for 5 h, mainly due to the change in V_{oc}, and then saturated. The improvement in V_{oc} is probably because Si dangling bonds created on the a-Si:H/c-Si interfaces during high-temperature processes such as B Cat-doping are terminated by H atoms supplied from a-Si:H during postannealing. J_{sc} slightly increased by postannealing for 5 h and then saturated. The slight improvement in J_{sc} is probably due to the suppressed carrier recombination on the Si surfaces and resulting more efficient collection of minority carriers. FF did not change significantly. As a result, in the case of B Cat-doping with H_2, the SHJ cell showed η = 12.6%, J_{sc} = 32.7 mA/cm^2, V_{oc} = 617 mV, FF = 0.625 after postannealing at 200 °C for 5 h. In the case of B Cat-doping without H_2, SHJ solar cells with a B Cat-doped a-Si:H layer showed less values of η = 10.8%, J_{sc} = 32.7 mA/cm^2, V_{oc} = 582 mV, FF = 0.568. The difference in the performance between the SHJ cells may be brought by more effective doping of B atoms on a-Si:H by the addition of H_2. Note that the performances of the SHJ solar cells with a B Cat-doped layer are

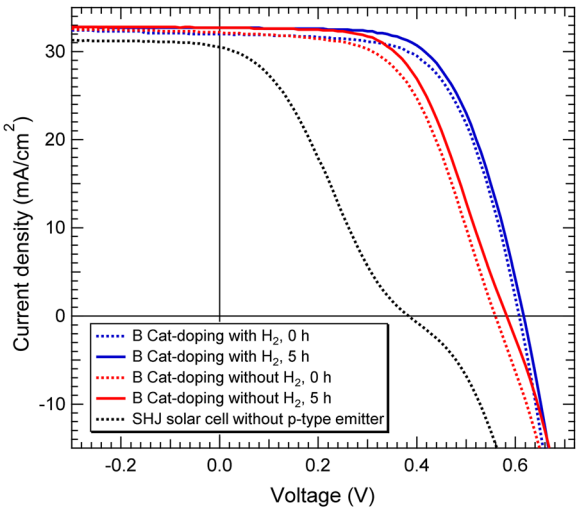

FIG. 5. *J–V* characteristics of SHJ solar cells with and without a B Cat-doped a-Si:H layer.

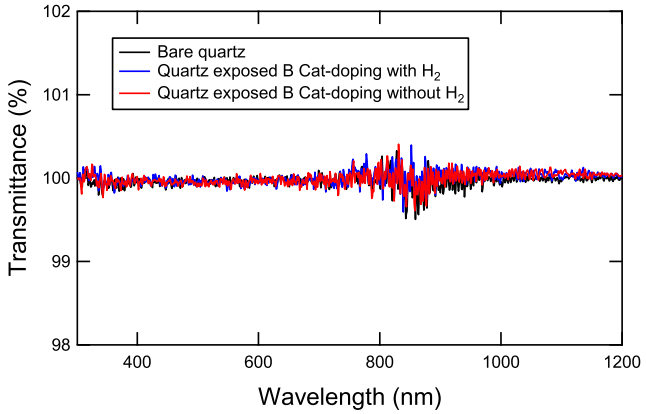

FIG. 6. Optical transmittance spectra of quartz glass substrates with and without exposure to B Cat-doping.

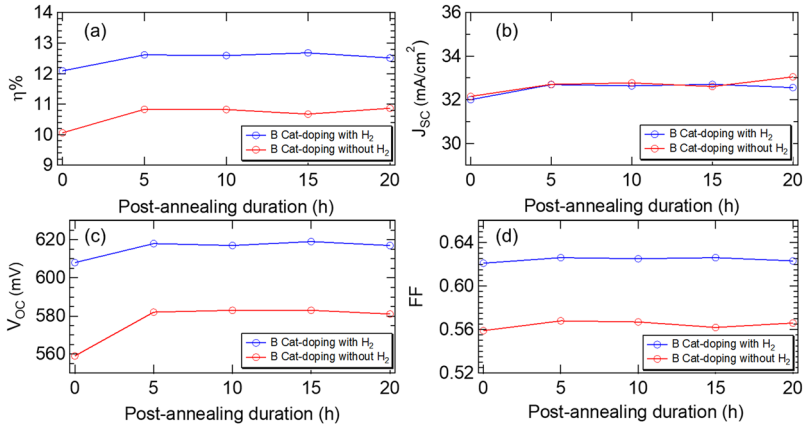

FIG. 7. (a) η, (b) J_{sc}, (c) V_{oc}, and (d) FF of the SHJ solar cells as a function of postannealing duration. Blue and red lines indicate the values of the SHJ cells with B Cat-doped a-Si:H layers formed with and without the addition of H_2, respectively.

much better than those of a SHJ cell with a B Cat-doped layer, which we have reported previously,[17] and are comparable to those of SHJ cells using deposited p-a-Si:H films fabricated in our group.[13,26,30]

In this study, we have demonstrated the feasibility of B Cat-doping to form a p-a-Si:H emitter layer for conventional SHJ solar cells. If the B Cat-doping is performed on an a-Si:H film through a hard mask, pattered p-a-Si:H regions may be partially formed without photolithography. The Cat-doping process may thus be applicable to the simple formation process of patterned doping regions in HBC solar cells.

IV. CONCLUSIONS

We investigated the improvement in the tunneling conduction through the ITO/B Cat-doped a-Si:H interfaces and the performance of SHJ cells with a B Cat-doped a-Si:H layer. ITO films deposited at 200 °C and B Cat-doped a-Si:H films with H_2 provide effective carrier tunneling through the ITO/a-Si:H interfaces. SHJ solar cells with a B Cat-doped a-Si:H layer with the addition of H_2 during B Cat-doping show better performance than those without H_2 addition. The postannealing of the SHJ cells for 5 h improves V_{oc} and η. As a result, in the case of B Cat-doping with H_2, we demonstrated SHJ solar cells with a B Cat-doped a-Si:H layer with η = 12.6%, J_{sc} = 32.7 mA/cm^2, V_{oc} = 617 mV, FF = 0.625. The p-a-Si:H formation by B Cat-doping will be applied to the fabrication process of HBC solar cells.

ACKNOWLEDGMENTS

This work was supported by JSPS KAKENHI, Grant No. 16K14400.

REFERENCES

[1] K. Yoshikawa, H. Kawasaki, W. Yoshida, T. Irie, K. Konishi, K. Nakano, T. Uno, D. Adachi, M. Kanematsu, H. Uzu, and K. Yamamoto, Nat. Energy **2**, 17032 (2017).
[2] M. Taguchi, A. Yano, S. Tohoda, K. Matsuyama, Y. Nakamura, T. Nishiwaki, K. Fujita, and E. Maruyama, IEEE J. Photovoltaics **4**, 96 (2014).
[3] K. Masuko, M. Shigematsu, T. Hashiguchi, D. Fujishima, M. Kai, N. Yoshimura, T. Yamaguchi, Y. Ichihashi, T. Mishima, N. Matsubara, T. Yamanishi, T. Takahama, M. Taguchi, E. Maruyama, and S. Okamoto, IEEE J. Photovoltaics **4**, 1433 (2014).
[4] T. F. Schulze, L. Korte, E. Conrad, M. Schmidt, and B. Rech, J. Appl. Phys. **107**, 023711 (2010).
[5] Z. C. Holman, A. Descoeudres, L. Barraud, F. Z. Fernandez, J. P. Seif, S. D. Wolf, and C. Ballif, IEEE J. Photovoltaics **2**, 7 (2012).
[6] J. Pia, M. Tamasi, R. Rizzoli, M. Losurdo, E. Centurioni, C. Summonte, and F. Rubinelli, Thin Solid Films **425**, 185 (2003).
[7] M. Taguchi, K. Kawamoto, S. Tsuge, T. Baba, H. Sakata, M. Morizane, K. Uchihashi, N. Nakamura, S. Kiyama, and O. Oota, Prog. Photovoltaics: Res. Appl. **8**, 503 (2000).
[8] M. A. Green, Y. Hishikawa, E. D. Dunlop, D. H. Levi, J. H. Einger, and A. W. Y. Ho-Baillie, Prog. Photovoltaics: Res. Appl. **26**, 3 (2018).
[9] H. Matsumura, M. Miyamoto, K. Koyama, and K. Ohdaira, Sol. Energy Mater. Sol. Cells **95**, 797 (2011).
[10] T. Hayakawa, T. Ohta, Y. Nakashima, K. Koyama, K. Ohdaira, and H. Matsumura, Jpn. J. Appl. Phys., Part 1 **51**, 101301 (2012).
[11] T. Ohta, K. Koyama, K. Ohdaira, and H. Matsumura, Thin Solid Films **575**, 92 (2015).
[12] H. Matsumura, T. Hayakawa, T. Ohta, Y. Nakashima, M. Miyamoto, T. C. Thi, K. Koyama, and K. Ohdaira, J. Appl. Phys. **116**, 114502 (2014).
[13] S. Tsuzaki, K. Ohdaira, T. Oikawa, K. Koyama, and H. Matsumura, Jpn. J. Appl. Phys., Part 1 **54**, 072301 (2015).
[14] T. C. Thi, K. Koyama, K. Ohdaira, and H. Matsumura, J. Appl. Phys. **116**, 044510 (2014).
[15] T. C. Thi, K. Koyama, K. Ohdaira, and H. Matsumura, Jpn. J. Appl. Phys., Part 1 **55**, 02BF09 (2016).
[16] J. Seto, K. Ohdaira, and H. Matsumura, Jpn. J. Appl. Phys., Part 1 **55**, 04ES05 (2016).
[17] K. Ohdaira, J. Seto, and H. Matsumura, Jpn. J. Appl. Phys., Part 1 **56**, 08MB06 (2017).
[18] H. Matsumura, Jpn. J. Appl. Phys., Part 1 **37**, 3175 (1998).
[19] H. Matsumura, J. Appl. Phys. **65**, 4396 (1989).
[20] H. Matsumura, Thin Solid Films **395**, 1 (2001).
[21] M. Itoh, Y. Ishibashi, A. Masuda, and H. Matsumura, Thin Solid Films **395**, 138 (2001).
[22] H. Matsumura, H. Umemoto, A. Izumi, and A. Masuda, Thin Solid Films **430**, 7 (2003).
[23] A. Masuda, C. Niikura, Y. Ishibashi, and H. Matsumura, Sol. Energy Mater. Sol. Cells **66**, 259 (2001).
[24] Y. Nozaki, M. Kitazoe, K. Horii, H. Umemoto, A. Masuda, and H. Matsumura, Thin Solid Films **395**, 47 (2001).
[25] K. Koyama, N. Yamaguchi, D. Hironiwa, H. Suzuki, K. Ohdaira, and H. Matsumura, Jpn. J. Appl. Phys., Part 1 **56**, 08MB21 (2017).

[26]T. Oikawa, K. Ohdaira, K. Higashimine, and H. Matsumura, "Application of crystalline silicon surface oxidation to silicon heterojunction solar cells," Curr. Appl. Phys. **15**, 1168 (2015).
[27]H. Kim, C. M. Gilmore, A. Pique, J. S. Horwitz, H. Mattoussi, H. Murata, Z. H. Kafafi, and D. B. Chrisey, J. Appl. Phys. **86**, 6451 (1999).
[28]H. Fujiwara and M. Kondo, J. Appl. Phys. **101**, 054516 (2007).
[29]H. Umemoto, T. Kanematsu, and A. Tanaka, J. Phys. Chem. A **118**, 5156 (2014).
[30]K. Ohdaira, T. Oikawa, K. Higashimine, and H. Matsumura, Curr. Appl. Phys. **16**, 1026 (2016).